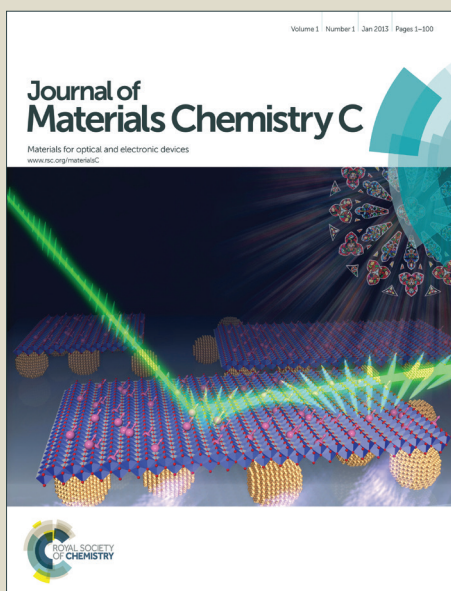


# Journal of Materials Chemistry C

Accepted Manuscript



This is an *Accepted Manuscript*, which has been through the Royal Society of Chemistry peer review process and has been accepted for publication.

*Accepted Manuscripts* are published online shortly after acceptance, before technical editing, formatting and proof reading. Using this free service, authors can make their results available to the community, in citable form, before we publish the edited article. We will replace this *Accepted Manuscript* with the edited and formatted *Advance Article* as soon as it is available.

You can find more information about *Accepted Manuscripts* in the [Information for Authors](#).

Please note that technical editing may introduce minor changes to the text and/or graphics, which may alter content. The journal's standard [Terms & Conditions](#) and the [Ethical guidelines](#) still apply. In no event shall the Royal Society of Chemistry be held responsible for any errors or omissions in this *Accepted Manuscript* or any consequences arising from the use of any information it contains.

# Strain-tunable magnetic properties of epitaxial lithium ferrite thin film on $\text{MgAl}_2\text{O}_4$ substrates

Ruyi Zhang, Ming Liu<sup>\*</sup>, Lu Lu, Shao-Bo Mi, Hong Wang<sup>\*</sup>

Electronic Materials Research Laboratory, Key Laboratory of the Ministry of Education & State Key Laboratory for Mechanical Behavior of Materials, Xi'an Jiaotong University, Xi'an 710049, P. R. China

Epitaxial  $\text{LiFe}_5\text{O}_8$  thin films with various thicknesses were fabricated on (001)  $\text{MgAl}_2\text{O}_4$  substrates by using a high-pressure sputtering system. All the  $\text{LiFe}_5\text{O}_8$  thin films have excellent epitaxial quality with ordered  $\alpha$ - $\text{LiFe}_5\text{O}_8$  structure, and larger in-plane compressive and out-of-plane tensile strain can be obtained by decreasing the film thickness. Moreover, the in-plane compressive strain can significantly induce the enhancement of in-plane magnetization while the out-of-plane tensile strain tends to reduce the out-of-plane magnetization. It indicates that controlling the thickness of the films is an effective method to tailor the interface strain and further modify the magnetic properties of the epitaxial  $\text{LiFe}_5\text{O}_8$  thin films.

---

<sup>\*</sup> Electronic address: [m.liu@mail.xjtu.edu.cn](mailto:m.liu@mail.xjtu.edu.cn); [hwang@mail.xjtu.edu.cn](mailto:hwang@mail.xjtu.edu.cn).

## 1. Introduction

Spinel phase lithium ferrite ( $\text{LiFe}_5\text{O}_8$  (LFO)) and its substitutions have drawn decades of research interest for their excellent physical properties in dielectric and magnetic aspects. The highest Curie temperature ( $\sim 950\text{K}$ ) in spinel ferrites, large resistivity, low eddy-current loss, narrow linewidth and thermal stability make lithium ferrite suitable candidate for high frequency applications and other new concept devices.<sup>1-4</sup> Normally,  $\text{LiFe}_5\text{O}_8$  possesses a structure of inverse spinel phase (denoted as  $\text{Fe}[\text{Li}_{0.5}^{+}\text{Fe}_{1.5}^{3+}]\text{O}_4$ ) with two fifth of all  $\text{Fe}^{3+}$  ions distributing in tetragonal sites (also known as 8a sites) and the rest  $\text{Fe}^{3+}$  and  $\text{Li}^{+}$  ions occupying the octahedral sites (16d sites). The occupation of  $\text{Li}^{+}$  and  $\text{Fe}^{3+}$  ions at the octahedral will form complex order and disorder structures and induced various interesting physical properties, such as its magnetocrystalline anisotropy and crystalline field parameters.<sup>5-7</sup> Moreover, the spin antiparallel of  $\text{Fe}^{3+}$  ions between 8a sites and 16d sites causes the ferrimagnetic features of lithium ferrite with a net molecular magnetic moment of  $2.5 \mu\text{B}$  per unit.

Interface engineering has become one of the most important techniques in tuning the microstructure and physical properties of multifunctional complex oxide thin films and nano-scale materials. In other words, many novel electrical and magnetic properties can be achieved by the interface modification.<sup>8-15</sup> Normally, one of the easiest yet effective ways to tailor the interface strain is the controlling of film thickness.<sup>16</sup> Many works have been reported on magnetic properties modified by interface strain. S. Kale *et al.* investigated the magnetization, conversion-electron Mössbauer, and ferromagnetic resonance of  $\text{Fe}_3\text{O}_4$  films of various thicknesses and discussed the contribution of strain to these properties.<sup>17</sup> Thickness dependence of structure and magnetization of  $\text{BiFeO}_3$  films were studied by D. S. Rana *et al.* and they found a weak enhancement of magnetization in fully strained films.<sup>18</sup> A large strain induced enhancement in  $T_c/T_{\text{IM}}$  was observed and discussed by R. Prasad *et al.* in

$\text{La}_{0.88}\text{Sr}_{0.12}\text{MnO}_3$  film with various thicknesses.<sup>19</sup> In lithium ferrite, however, few works have been focused on the thickness dependent interface strain and magnetic properties of LFO highly epitaxial thin films.<sup>20-22</sup>

In this paper, the epitaxial LFO thin films with various thicknesses have been grown on (001)  $\text{MgAl}_2\text{O}_4$  (MAO) substrates by using high-pressure sputtering system. We have systematically investigated the relationship between the interface strain and magnetic properties. It is found that the interface strain can significantly tune the magnetic properties of the LFO epitaxial thin films.

## 2. Experimental

A high-pressure sputtering system had been used to fabricate the LFO thin films. The stoichiometric  $\text{LiFe}_5\text{O}_8$  ceramic target was prepared through standard solid state reaction method with initial reactants  $\text{LiCO}_3$  and  $\text{Fe}_2\text{O}_3$  (ratio 2:5). Before the thin film deposition, the target was pre-sputtered for 12 hours to eliminate potential contaminant on the surface. The MAO substrates have been used to grow LFO films, which have a similar structure and relatively small lattice mismatch ( $\sim 2.95\%$ ) with lithium ferrite materials (MAO substrate:  $a = 8.085 \text{ \AA}$ ; LFO bulk material:  $a = 8.331 \text{ \AA}$ ). The optimized deposition condition for epitaxial growth was achieved at the substrate temperature of  $800 \text{ }^\circ\text{C}$  under working pressure of  $0.5 \text{ mbar}$  with the mixed ambient of Ar and  $\text{O}_2$  in the ratio of 1:1. In order to investigate the thickness effect on its microstructure and physical properties, the LFO thin films with various thicknesses of  $53 \text{ nm}$ ,  $27 \text{ nm}$ ,  $13 \text{ nm}$ , and  $7 \text{ nm}$  were fabricated. The crystallinity and epitaxial behavior of the LFO films were characterized by a high resolution x-ray diffraction (HRXRD) of PANalytical X'Pert MRD and a scanning transmission electron microscopy (STEM). The magnetic properties of the LFO thin films were evaluated by using a superconducting quantum interference device magnetometer (SQUID) measured along both

in-plane and out-of-plane direction at room temperature.

### 3. Results and discussion

The crystalline qualities of the LFO thin films were characterized by the XRD  $\theta$ - $2\theta$  scan,  $\varphi$  scan and reciprocal space mapping (RSM). Fig. 1a is the typical wide angle  $\theta$ - $2\theta$  patterns of the LFO thin films deposited on MAO (001) substrates with the film thicknesses of 7 nm and 53 nm. Only (004) reflections of LFO and MAO (00 $l$ ) reflections can be found, revealing that the LFO films only have one growth direction with no second phase. Fig. 1b depicts the detailed  $\theta$ - $2\theta$  patterns scans for all LFO films, showing the evolution of diffraction peaks as film thickness increases. It can be clearly seen that the LFO (004) peak shifts toward higher angles with the thickness increasing, indicating that the out-of-plane lattice parameter  $c$  of the LFO films decrease with the thickness increasing. This means a larger compressive strain of the films can be obtained with the thickness decreasing. The  $\varphi$  scan measurements have been used to understand the epitaxial nature and the in-plane interface relationship between the films and the substrates. As shown in the Fig. 1c, the  $\varphi$  scans are performed around the {101} reflections of the LFO films and the MAO substrates. The four-fold symmetry and sharp peaks in the  $\varphi$  scan pattern of the LFO films suggest that the films have good single crystallinity and excellent epitaxial nature. Therefore, the orientation relationship between the films and the substrates is determined to be  $[100]_{\text{LFO}}//[100]_{\text{MAO}}$  and  $(001)_{\text{MAO}}//(001)_{\text{STO}}$  from the  $\varphi$  scans.

It is well known that the reciprocal space mapping (RSM) technology is a very effective method to study the microstructure, such as lattice parameters, defect density and domain structure. To further understand the crystallographic evolution and the interface strain of LFO films with various thicknesses, the RSMs have been performed around the (004), (206) and (026) reflections of the LFO films and MAO substrates. Fig. 2a is the symmetric RSMs

recorded around from the (004) reflections of the LFO films and MAO substrates with the thickness of 7 nm to 53 nm. It can be seen that the diffraction angle of the (004) LFO peak decreases with the thickness decreasing, indicating that the out-of-plane lattice parameter  $c$  increases accordingly. Moreover, it corresponds to the results obtained from  $\theta$ - $2\theta$  scans. Fig. 2b-c are the asymmetric RSMs taken around from the (206) and (026) reflections of the LFO films and MAO substrates with various thicknesses. First, we measure the RSMs around (206) reflections along one of the in-plane axis, defining it as [100] direction with  $\varphi = 0^\circ$ . Then, the same measurements have been done but  $\varphi$  rotates  $90^\circ$ , which we defined as the RSMs of (026) along [010] direction. Thus, the in-plane lattice parameters ( $a$  and  $b$ ) of LFO films with various thicknesses are calculated and illustrated in Fig. 2d. From the tendencies of curves in Fig. 2d, it is found that the in-plane lattice constants of the films decrease and the out-of-plane lattice constants increase with the thickness decreasing from 53 nm to 7 nm. It reveals that the in-plane compressive strain and out-of-plane tensile strain gradually relax with the film thickness increasing. In other words, the LFO thin films are driven by a larger compressive strain along the in-plane direction with the thickness decreasing.

In order to further investigate the epitaxial behavior and the microstructure of the LFO films, the cross-sectional TEM studies have been performed on the LFO/MAO heterostructure. Fig. 3a is a low-magnification bright field TEM image and a selected-area electron diffraction (SAED) of the LFO/MAO (001) sample. The thickness of LFO film is about 53 nm and the LFO/MAO interface is sharp as denoted by a horizontal arrow. In addition, the interface between LFO film and Au capping layer is indicated by a horizontal arrow. The SAED pattern was recorded in the region including the LFO film and part of the MAO substrate. In the SAED pattern, apart from the strong diffraction spots contributed from the LFO film and the MAO substrate, the weak diffraction spots are from the LFO film. Accordingly, the film-substrate orientation relationship  $[100]_{\text{LFO}}//[100]_{\text{MAO}}$  and

$(001)_{\text{LFO}}// (001)_{\text{MAO}}$  can be determined, which is consistent with the results obtained by X-ray diffraction. On the basis of our TEM investigations, it can be concluded that single-crystal LFO film epitaxially grows on MAO substrate under our film growth conditions. Fig. 3b is a cross-sectional high-resolution TEM lattice image of the interface region viewed along the  $[110]$  zone axis of MAO. Misfit dislocations can be observed at the interface as denoted by a vertical arrow, indicating that the film-substrate strain has been relaxed when the film thickness is up to 53 nm. These dislocations form at the interface contributing to release the large interfacial energy caused by a  $\sim 2.95\%$  lattice misfit between film and substrate in thick film samples.<sup>23</sup>

Fig. 3c is a typical atomic-resolution high-angle annular dark-field STEM (HAADF-STEM) image of the LFO film, viewed along the  $[110]$  zone axis of LFO. The intensity variation of atomic columns is clearly visible. It is known that the intensity of the HAADF image is approximately proportional to the square of the mean atomic number  $Z$  in the atomic columns.<sup>24</sup> Fig. 3d shows the intensity profiles along the atomic rows marked by a red line in Fig. 3c. The intensity variation of the octahedral B sites in  $\text{LiFe}_5\text{O}_8$  was detected as shown by a green and a red arrow, respectively. It indicates that lithium and iron atoms in our LFO films are ordered at the octahedral B sites and  $\alpha\text{-LiFe}_5\text{O}_8$  structure forms in the LFO/MAO system under our film growth conditions.

In order to understand the influence of LFO film thickness on its magnetic properties, the magnetic hysteresis loops have been measured at room temperature by using a SQUID system. As the MAO substrate exhibits strong diamagnetism, it can't be ignored for the magnetic property measurements of the LFO thin films. Therefore, we measure the magnetic response of the bare MAO substrates (reference) and the MAO substrates with the LFO thin films (test samples), respectively. After the calculation, the intrinsic magnetic properties merely from LFO layer can be obtained. The M-H hysteresis loops measured along in-plane

and out-of-plane directions of 7nm-, 13nm-, 27nm-, and 53nm- thick LFO films are presented in Fig. 4a (1)-(4). To clearly demonstrate the variation tendency of saturation magnetization ( $M_s$ ) and coercivity with the increasing of film thickness, both of them have been plotted in the Fig. 4b. The in-plane saturation magnetization reaches the highest value of 172 emu/cc of 7nm- thick film and drops gradually to 154 emu/cc of 53 nm- thick film. Meanwhile, the out-of-plane magnetization increases with film thickness with highest value of 189 emu/cc of 53 nm- thick film. Therefore, the in-plane and out-of-plane saturation magnetization show a completely opposite variation tendency with the increase of film thickness. To explain this phenomenon of thickness dependent magnetic properties, we need to consider the influence of factors from a structural point of view. According to the results from XRD and TEM measurement, no obvious chemical composition change in our ordered LFO epitaxial films is observed. Therefore, we can rule out the possibility of cation redistributions between A and B sites, and some Fe rich regions in ultra-thin layer that may cause variations of magnetic properties in ferrite films.<sup>17, 25-27</sup> The most likely factor of tuning the magnetic properties in our system should be the interface strain due to lattice misfit between LFO film and MAO substrate. Magnetic properties tuned by strain can be understood from the magnetoelastic energy density which depicts the relationship between magnetic and mechanical parameters. To make the discussion simple, we firstly consider the in-plane magnetoelastic energy density which can be expressed as  $E_\sigma = -\frac{1}{2}\mu_0 H_{eff} M_s \sigma \cos^2 \theta = \frac{3}{2}\lambda_s \sigma \cos^2 \theta$ , where  $\lambda_s$  is the saturation magnetostriction,  $\sigma$  is the stress (which can be deduced from the strain by multiplying Young modulus of material),  $\theta$  is the angle between the magnetization and stress (which is zero for in-plane circumstances),  $H_{eff}$  is the effective magnetic anisotropy induced by strain. As LFO is negative magnetostrictive material with  $\lambda_s$  of -27.8 ppm, the in-plane compressive strain would enhance the in-plane magnetization by the change of in-plane effective magnetic anisotropy. The effective magnetic anisotropy by induced stress can be directly observed in

Fig. 4a, where larger in-plane compressive strain leads to the in-plane magnetic easy axis. In another words, the in-plane compressive strain is inclined to align the spin along the film plane. Similar way can also be used for the out-of-plane magnetization analysis, which is strongly affected by the out-of-plane tensile strain. The in-plane compressive strain (or out-of-plane tensile strain) induced in-plane (or out-of-plane) magnetization enhancement (or decrease), which is also observed in other similar negative magnetostrictive spinel ferrimagnetic system like zinc ferrite and cobalt ferrite published in recent years.<sup>26, 28, 29</sup> Moreover, it can be clearly seen that the coercivity increases with the thickness increasing (shown in the bottom graph of Fig. 4b). Coercivity is often treated as an extrinsic property of materials that is sensitive to the defects like metallurgical inhomogeneities, grain boundaries, and dislocations. We have presented a clear evidence of strain relaxation process as the LFO film thickness increases and the density of dislocations accumulates during this process. These dislocations can act as pinning centers and trap domain walls.<sup>30</sup> If these dislocations have very strong pinning effect on domain walls, they will give rise to high anisotropies and high coercivities. Thicker films with higher density of dislocations will have higher coercivity. Overall, the interface strain can be used to tune/control the microstructures and physical properties of the epitaxial LFO thin films, which are promising for the applications in strain tunable microwave devices.

#### 4. Conclusions

Ordered  $\alpha$ -LiFe<sub>5</sub>O<sub>8</sub> structural thin films with various thicknesses have been epitaxially grown on MAO (001) substrates by using a high-pressure sputtering system. The epitaxial LFO films show excellent single-crystalline quality with atomic sharp interface and a larger in-plane compressive strain (out-of-plane tensile strain) can be achieved with the thickness decreasing. In addition, the in-plane compressive strain (or out-of-plane tensile strain) can

significantly enhance the in-plane magnetization (or reduce the out-of-plane magnetization) and decrease the coercivity. The results indicate that controlling the thickness of the films is effective in tuning the interface strain and modifying the magnetic properties of the epitaxial LFO thin films.

### Acknowledgements

The work was supported by the National Natural Science Foundation of China (Nos: 61471290, 51390472 and 51202185), the SRFDP-RGC Joint Research Project 2013/14 (20130201140002) and National “973” projects of China (No. 2015CB654903). It was also partially supported by the Fundamental Research Funds for the Central University.

### Figure Captions

**Fig. 1** (a) A typical XRD wide angle  $\theta$ - $2\theta$  scans of 7nm- and 53nm- thick LFO/MAO (001) film samples; (b) Detailed  $\theta$ - $2\theta$  scans of all LFO films showing peak shifts due to interface strain; (c)  $\varphi$  scans taken around the {101} diffraction of the LFO films on (001) MAO substrates with the thickness of 53 nm.

**Fig. 2** Reciprocal space mappings taken around (004) (a), (206) (b), (026) (c) reflections, and calculated lattice parameters (in-plane and out-of-plane) and  $c/a$  ratio (d) for the LFO films with various thicknesses. Film thickness increases from 7nm in the leftmost graph to 53nm in the rightmost graph in (a)-(c).

**Fig. 3** (a) A low-magnification bright field TEM image of the LFO/MAO heterostructure and a selected-area electron diffraction (SAED) recorded at the film-substrate interface. The interfaces are indicated by horizontal arrows. (b) A high-resolution TEM lattice image of the LFO/MAO interface viewed along the [110] zone axis of MAO. Interfacial dislocations are indicated by a vertical arrow. (c) An atomic-resolution HAADF-STEM image of the LFO films, viewed along the [110] zone axis of LFO. (d) The intensity profiles taken along the atomic rows marked by a red line in (c). The atomic columns of the octahedral B sites in  $\text{LiFe}_5\text{O}_8$  with different intensity are indicated by a green and a red arrow, respectively.

**Fig. 4** (a) In-plane and out-of-plane magnetic hysteresis loops of LFO/MAO (001) films of different thicknesses measured at room temperature (300K). (b). Saturation magnetization ( $M_s$ ) and Coercivity as a function of film thickness.

## Notes and references

- 1 Argentin.Gm and P. D. Baba, *Microw. Theory Techn.*, 1974, **Mt22**, 652-658.
- 2 M. Sugimoto, *J. Am. Ceram. Soc.*, 1999, **82**, 269-280.
- 3 H. L. Glass, *Proc. IEEE*, 1988, **76**, 151-158.
- 4 M. Pardavi-Horvath, *J. Magn. Magn. Mater.*, 2000, **215**, 171-183.
- 5 E. Wolska, P. Piszora, W. Nowicki and J. Darul, *Int. J. Inorg. Mater.*, 2001, **3**, 503-507.
- 6 V. J. Folen, *J. Appl. Phys.*, 1960, **31**, S166-S167.
- 7 J. Dash, R. Krishnan, N. Venkataramani, S. Prasad, S. N. Shringi, P. Kishan and N. Kumar, *J. Magn. Magn. Mater.*, 1996, **152**, L1-L4.
- 8 M. Liu, C. Ma, G. Collins, J. Liu, C. Chen, C. Dai, Y. Lin, L. Shui, F. Xiang, H. Wang, J. He, J. Jiang, E. I. Meletis and M. W. Cole, *ACS Appl. Mater. Interfaces*, 2012, **4**, 5761-5765.
- 9 M. Liu, Q. Zou, C. Ma, G. Collins, S. B. Mi, C. L. Jia, H. Guo, H. Gao and C. Chen, *ACS Appl. Mater. Interfaces*, 2014, **6**, 8526-8530.
- 10 C. Ma, M. Liu, G. Collins, H. Wang, S. Bao, X. Xu, E. Enriquez, C. Chen, Y. Lin and M. H. Whangbo, *ACS Appl. Mater. Interfaces*, 2013, **5**, 451-455.
- 11 H. S. Kim, L. Bi, D. H. Kim, D. J. Yang, Y. J. Choi, J. W. Lee, J. K. Kang, Y. C. Park, G. F. Dionne and C. A. Ross, *J. Mater. Chem.*, 2011, **21**, 10364-10369.
- 12 F. Guoli, X. Xu, F. Jun and L. Feng, *J. Mater. Chem.*, 2010, **20**, 7378-7385.
- 13 S. R. Naik and A. V. Salker, *J. Mater. Chem.*, 2012, **22**, 2740-2750.
- 14 C. Ma, M. Liu, C. L. Chen, Y. Lin, Y. R. Li, J. S. Horwitz, J. C. Jiang, E. I. Meletis and Q. Y. Zhang, *Sci. Rep.*, 2013, **3**, 3092.
- 15 C. Ma, M. Liu, G. Collins, J. Liu, Y. Zhang, C. Chen, J. He, J. Jiang and E. I. Meletis, *App. Phys. Lett.*, 2012, **101**, 021602.
- 16 V. Nagarajan, S. Prasertchoung, T. Zhao, H. Zheng, J. Ouyang, R. Ramesh, W. Tian, X. Q. Pan, D. M. Kim, C. B. Eom, H. Kohlstedt and R. Waser, *Appl. Phys. Lett.*, 2004, **84**, 5225.
- 16 S. Kale, S. M. Bhagat, S. E. Lofland, T. Scabarozzi, S. B. Ogale, A. Orozco, S. R. Shinde, T. Venkatesan, B. Hannoyer, B. Mercey and W. Prellier, *Phys. Rev. B*, 2001, **64**, 205413.
- 18 D. S. Rana, K. Takahashi, K. R. Mavani, I. Kawayama, H. Murakami, M. Tonouchi, T. Yanagida, H. Tanaka and T. Kawai, *Phys. Rev. B*, 2007, **75**, 060405.
- 19 R. Prasad, H. K. Singh, M. P. Singh, W. Prellier, P. K. Siwach and A. Kaur, *J. Appl. Phys.*, 2008, **103**, 083906.
- 20 S. A. Oliver, C. Vittoria, G. Balestrino, S. Martellucci, G. Petrocelli, A. Tebano and P. Paroli, *IEEE Trans. Magn.*, 1994, **30**, 4933-4935.
- 21 G. Balestrino, S. Martellucci, A. Paoletti, P. Paroli, G. Petrocelli, A. Tebano, S. A. Oliver and C. Vittoria, *Micros. Technol.*, 1995, **1**, 115-120.
- 22 C. Boyraz, D. Mazumdar, M. Iliev, V. Marinova, J. X. Ma, G. Srinivasan and A. Gupta, *Appl. Phys. Lett.*, 2011, **98**, 012507.
- 23 Y. Lin and C. L. Chen, *J. Mater. Sci.*, 2009, **44**, 5274-5287.
- 24 S. J. Pennycook, B. Rafferty and P. D. Nellist, *Microsc. Microanal.*, 2000, **6**, 343-352.
- 25 U. Lüders, M. Bibes, J.-F. Bobo, M. Cantoni, R. Bertacco and J. Fontcuberta, *Phys. Rev. B*, 2005, **71**, 134419.
- 26 S. C. Sahoo, N. Venkataramani, S. Prasad, M. Bohra and R. Krishnan, *Appl. Phys. A*, 2011, **106**, 931-935.
- 27 J. Moyer, C. Vaz, D. Kumah, D. Arena and V. Henrich, *Phys. Rev. B*, 2012, **86**, 174404.
- 28 Y. J. Yang, M. M. Yang, Z. L. Luo, C. S. Hu, J. Bao, H. L. Huang, S. Zhang, J. W. Wang, P. S. Li, Y. Liu, Y. G. Zhao, X. C. Chen, G. Q. Pan, T. Jiang, Y. K. Liu, X. G. Li and C. Gao, *J. Appl. Phys.*, 2014, **115**.
- 29 J. M. Iwata, R. V. Chopdekar, F. J. Wong, B. B. Nelson-Cheeseman, E. Arenholz and Y. Suzuki, *J. Appl. Phys.*, 2009, **105**, 07A905.
- 30 Y. Liu, D. J. Sellmyer and D. Shindo, *Handbook of Advanced Magnetic Materials: Vol 1. Nanostructural Effects*, Springer Science+Business Media, New York, 2005.

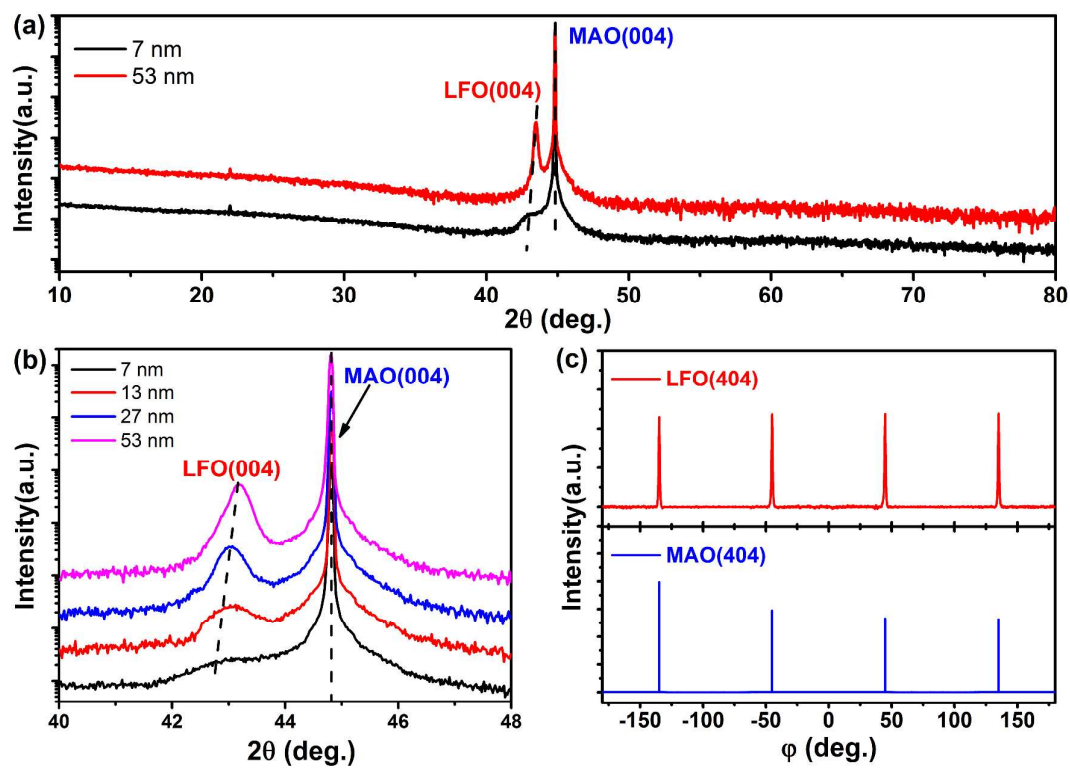


Figure 1

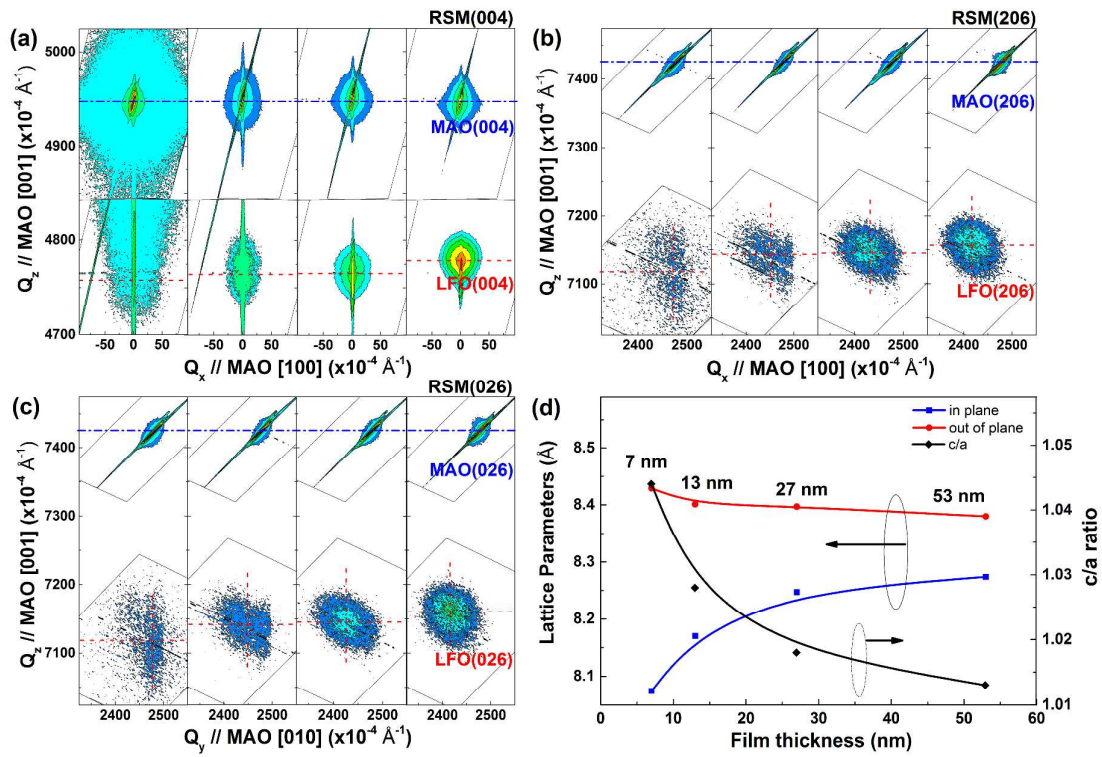


Figure 2

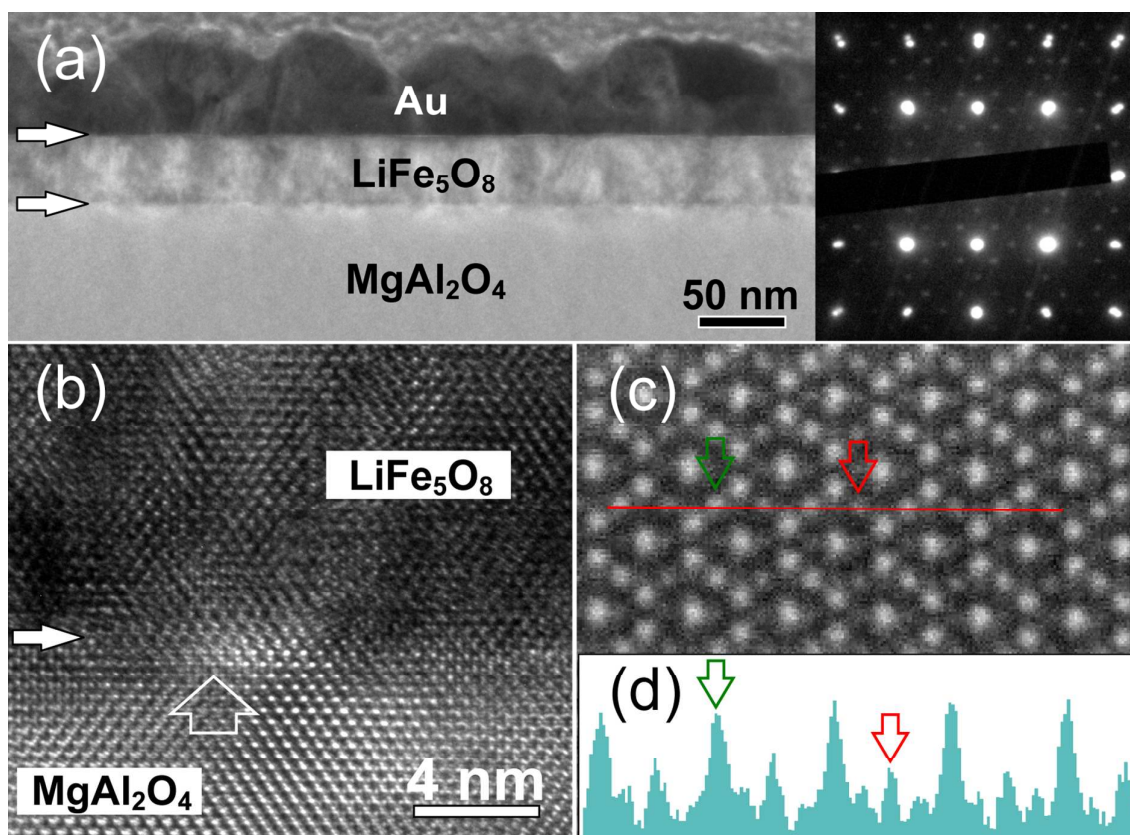


Figure 3

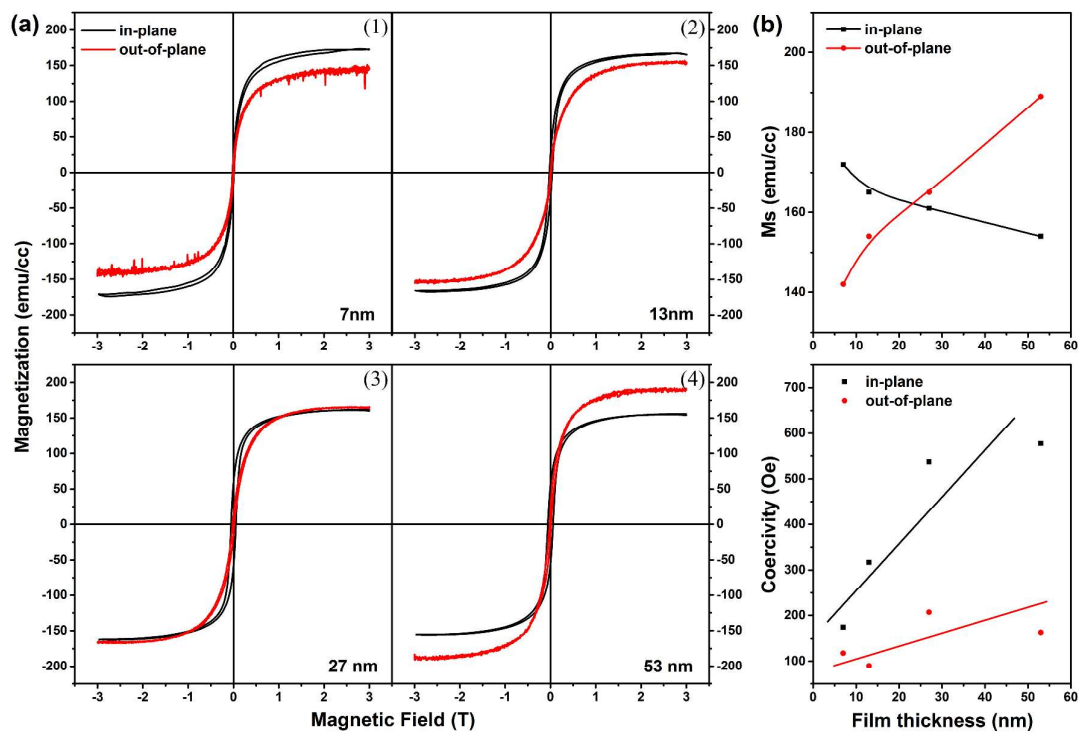


Figure 4

Interface engineering by the controlling of film thickness is an effective method to tune/control the magnetic properties of epitaxial  $\text{LiFe}_5\text{O}_8$  thin films fabricated by a high-pressure sputtering system.

